Arnold Vainrub
B. Montgomery Pettitt
Department of Chemistry, University of Houston, Houston, TX 77204-5003

Received 23 April 2002; accepted 30 July 2002

Surface Electrostatic Effects in Oligonucleotide Microarrays: Control and Optimization of Binding Thermodynamics

Abstract: *We present a theoretical thermodynamic framework for the design of more efficient oligonucleotide microarrays. A general thermodynamic relation is derived to describe the electrostatic surface effects on the binding of the assayed biomolecule to a surface-tethered molecular probe. The relation is applied to analyze how the nucleic acid target, the oligonuleotide probe, and their DNA duplex electrostatic interactions with the surface affect the hybridization on DNA arrays. Taking advantage of a closed form exact solution of the linear Poisson–Boltzmann equation for a charged ion-penetrable sphere in electrolyte solution interacting with a plane wall, we study the effects of the surface and solution conditions. Binding free energy is found as a function of the surface material, dielectric or metal, the surface charge density, linker molecule length, temperature, and added salt content. The charge or electric potential of the dielectric or metal surface, respectively, is shown to dominate the hybridization, especially at low added salt or short linker length. We predict that substantial enhancement of sensitivity, selectivity, and reliability of microarrays can be achieved by control of the surface conditions. As examples, we discuss how to overcome two limitations of current technologies: nonequal sensitivity of the probes with different GC and AT bases content, and poor match/mismatch discrimination. In addition, we suggest the design of microarray conditions where the tested nucleic acid is unfolded, thus making possible the screening of a larger sequence with single nucleotide resolution. These promising findings are discussed and further experimental tests suggested.* © 2003 Wiley Periodicals, Inc. Biopolymers 68: 265–270, 2003

Keywords: *theoretical thermodynamics; oligonucleotide microarrays; electrostatic surface effects*

INTRODUCTION

Progress in DNA microarray technologies depends on improvement of their sensitivity, selectivity, and reliability.[1,2] So far these parameters have been optimized essentially empirically as a result of many experimental efforts.[3–5] Based on our previous theoretical analysis of the surface electrostatic effects,[6] which is in accord with recent experiments,[7] we describe here the effect of the surface charge density on the melting curve and match/mismatch discrimination ratio for surface hybridization, and predict possible substantial improvements in several properties for microarrays. The surface material, dielectric or metal,

Correspondence to: B. Montgomery Pettitt; email: pettit@uh.edu

Contract grant sponsor: NIH, Texas Higher Education Coordinating Board, and Robert A. Welch Foundation

Biopolymers, Vol. 68, 265–270 (2003)

and the surface electrostatic conditions are shown to be critically important because they strongly determine the yield of the nucleic acid target hybridization to the surface-immobilized oligonucleotide probes. We propose to use these properties for control and enhancement of sensitivity during surface hybridization. In particular, an equal sensitivity of the probes with different base-pair composition may be achieved by adjustment of their specific linker molecule length or the local surface charge. Further, we suggest enhancement of the match/mismatch discrimination by narrowing the melting curve by optimizing the surface charge. Finally, we discuss a new microarray design using hybridization at low salt where the duplex stability is achieved by the positive surface charge. Under these conditions the target's secondary structure is melted, allowing hybridization to most of the target's nucleotides and increasing the sequencing information up to tenfold.

THEORETICAL MODEL AND CALCULATION METHODS

Oligonucleotide–surface interaction free energy was evaluated using the linear Poisson–Boltzmann (PB) model for an ion-penetrable charged sphere and plate immersed in an electrolyte solution. The use of linear PB theory must be justified a posteriori as the conditions for validity are not always clear. Previous work has shown that this theoretical framework has qualitative validity for this system,[6] and we present experimental quantitative comparisons below. The ion-penetrable charged sphere model of very short duplex oligonucleotides has been shown to be reasonable as an average picture in comparison with atomic simulations.[10] An exact solution of this model obtained by Oshima[8] was utilized to calculate the Gibbs free energy of the interaction as described in Ref. 6. The surface potential was chosen to be near the normally accepted range of validity of linearized PB theory, which is limited to roughly 26 mV corresponding to the electrostatic energy for a singly charged ion being equal to the room temperature thermal energy. Calculations were performed for a CAGGTTAT/GTCCAATA duplex using its hybridization enthalpy and entropy measured in solution.[9] The 8 base-pair fragment of DNA helix with a height of 2.4 nm and diameter of 2 nm was approximated by a 1 nm radius sphere bearing a negative surface charge $q = -16e$. The sphere contained electrolyte solution to model a penetration of ions and solvent into the deep hydrophilic grooves of the double helix as seen in simulation and experiment.[10]

RESULTS AND DISCUSSION

Statistical Thermodynamics of Hybridization

Understanding the experimentally well-established differences[3,4,11] in hybridization behavior between free probes in solution and surface-tethered probes is of central importance for optimizing DNA microarrays. A direct statistical thermodynamics approach is convenient for this analysis. We consider the surface effects using the general formula for the equilibrium in a reversible first-order chemical reaction[12]

$$n = 1/[1 + C_0^{-1} \exp(\Delta G/RT)], \quad (1)$$

where n is the fraction of the hybridized probes in equilibrium, C_0 is the concentration of the targets, and ΔG is the molar Gibbs free energy of the probe:target duplex formation. Equation (1) is valid under the condition that the target concentration is constant. For brevity, we omit a straightforward derivation for a general case when targets are depleted because of hybridization. Note that at constant temperature Eq. (1) corresponds to the well-known Langmuir adsorption isotherm equation, which is often used to interpret microarray experiments.[3] For discussing the mechanism of the interaction below, we introduce here the interaction Gibbs free energy with the surface for the probe V_p, target V_t, and duplex V_d. This interaction impacts the hybridization equilibrium and therefore the parameters in Eq. (1) in several ways. First, the target concentrations on the surface C_s and in solution C_0 vary according to the Boltzmann distribution formula

$$C_s = C_0 \exp(-V_t/RT) \quad (2)$$

Second, the Gibbs free energy differences of the duplex formation on the surface ΔG_s and in solution ΔG differ by the change of the interaction energy after and before hybridization, $(V_d - V_p - V_t)$. Thus

$$\Delta G_s = \Delta G + V_d - V_p - V_t \quad (3)$$

Equations 2 and 3 account for the target concentration and duplex binding strength changes near the surface, respectively. Substitution of Eqs. (2) and (3) in Eq. (1) gives the formula

$$n_s = 1/\{1 + C_0^{-1} \exp[(\Delta G + V_d - V_p)/RT]\}, \quad (4)$$

which describes the effect of surface interactions on the hybridization equilibrium. This equation differs from Eq. (1) for hybridization in bulk by addition of $(V_d - V_p)$ to the hybrid formation free energy. Hence, if duplex and probe are attracted to the surface ($V_d < 0$ and $V_p < 0$), the stronger attraction of the duplex for the surface $|V_d| > |V_p|$ promotes duplex formation. In contrast, a stronger surface repulsion of the duplex than the probe shifts the hybridization equilibrium toward melting of duplexes into single strand targets and probes.

This approach can be also used out of thermodynamic equilibrium when the target's concentration on the surface C_s is determined not by the Boltzmann distribution Eq. (2), but rather by some steady state transport process. The corresponding C_s and Eq. (3) should be substituted in Eq. (1) to obtain the equilibrium yield of the duplexes in surface hybridization, n_s. This is relevant to electronic DNA chips where the assayed nucleic acid is transported by electrokinetic drag[13,14] and flow-through biochips.[15]

Surface Electrostatic Interaction

In order to evaluate the hybridization with the surface tethered probes, one need to know the probe V_p and duplex V_d interaction energies in Eq. (4). Recently, we calculated the oligonucleotide–surface interaction in electrolyte solution.[6] We assumed the electrostatic interaction to be dominant since in microarray applications typically the oligonucleotide is tethered to the surface through a sufficiently long linker molecule, making the short-range van der Waals forces weak and therefore their effect small. The electrostatic Gibbs free energy was shown to be a sum of two components, V_1 and V_2. As depicted in Figure 1, V_1 corresponds to the direct electrostatic interaction with the surface charge and is attractive (repulsive) for the positively (negatively) charged surface because of the negative charge of the nucleic acid target. V_2 is the target's electrostatic free energy of interaction with uncharged dielectric or zero potential metallic surfaces. This part of the interaction is calculated by the method of images and is represented by an interaction with a fictitious image charge. For a metallic surface, V_2 is attractive; the image charge is of the same magnitude but has an opposite sign to the target's charge. For the dielectric surface, the magnitude of the free energy of interaction clearly depends on the dielectric constant. However, in practical terms the dielectric constant of surface material is low compared to the relatively high dielectric constant of water where $\epsilon = 80$. This allows one to view the image interaction with different dielectric surfaces as a repulsion from the image charge, which is equal to the target's charge. The Coulomb screening in the electrolyte solution further causes essentially exponential decay of electric interactions with the distance as $V_1 \sim \exp(-\kappa h)$ and $V_2 \sim \exp(-2\kappa h)$, where κ is the inverse Debye screening radius. Note that V_2 decays faster than V_1 since the target-image distance in Figure 1A is twice the target-surface distance h.

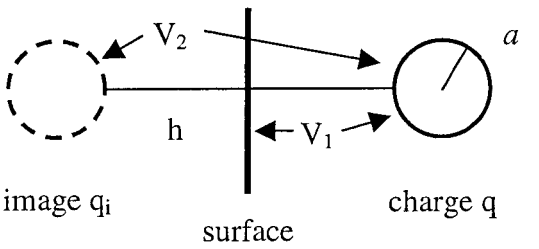

FIGURE 1 Electrostatic nucleic acid–surface interaction in electrolyte solution is presented by the sum of the charge q with the surface charge V_1 and charge–image charge interactions V_2. V_1 is attractive (repulsive) for the positively (negatively) charged surface, respectively, because of the negative charge of nucleic acid target. For a metal surface the image charge $q_i = -q$ and provides an attractive V_2, whereas for a dielectric surface $q_i = q$ and the interaction V_2 is repulsive.

DNA Duplex Melting Temperature

The hybridization thermodynamics of perfectly matched CAGGTTAT/GTCCAATA duplex on the surface was evaluated according to the theoretical method developed in Ref. 6. As is standard, the duplex stability is expressed in terms of the melting temperature T_m defined at equilibrium as the temperature at which half of the probes form duplexes [$n_s = 0.5$ in Eq. (4)]. Figure 2 demonstrates the shift of T_m on the surface relative to the bulk as a function of the probe–surface distance. The results are given for dielectric (upper row) and metallic (bottom row) surfaces for hybridization at four NaCl salt concentrations from 1 mM to 1M.

As shown in Figure 2, for an uncharged dielectric surface the melting temperature is reduced compared to its value in solution far from the surface. In contrast, a zero potential metallic surface increases the melting temperature. This different behavior is in accordance with the above-mentioned repulsive and attractive nature of the image interaction V_2, with dielectrics and metals, respectively. The positive surface charge ($\Phi = +25$ mV) introduces an attractive V_1 interaction and increases the melting temperature above that at a neutral surface. Since the decay length

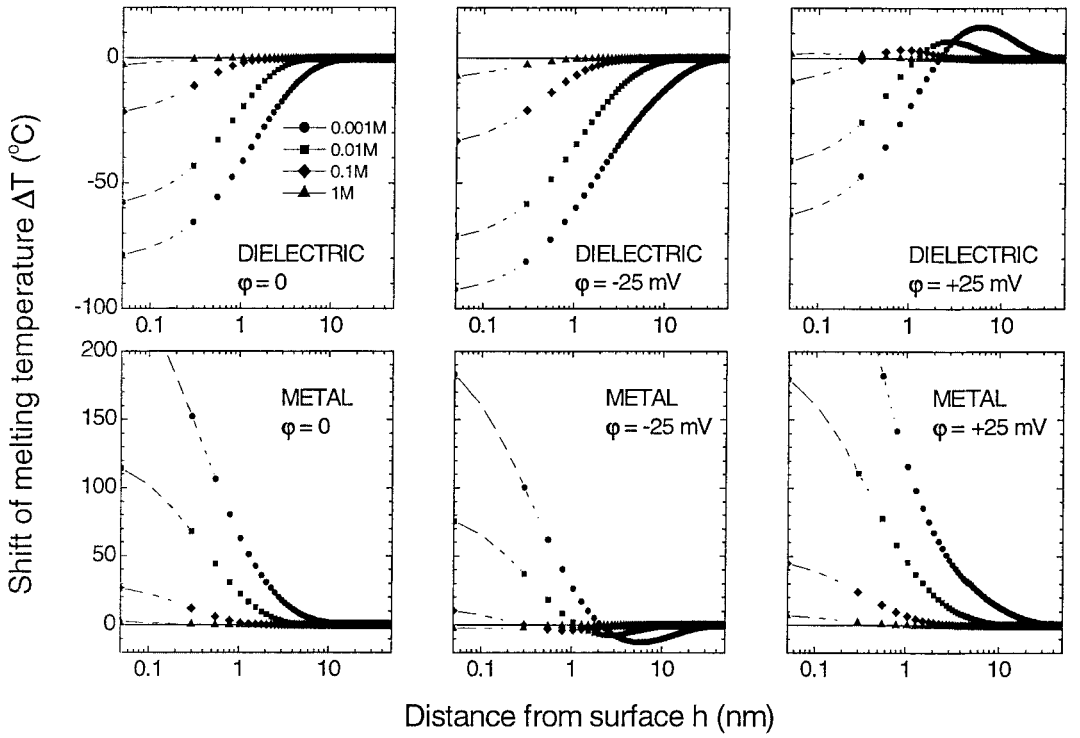

FIGURE 2 Probe–surface distance dependence of the melting temperature shift for the CAGGTTAT/GTCCAATA duplex at various NaCl concentrations from 0.001 to 1*M* as indicated. The metallic surface (bottom row) tends to increase the melting temperature because of the attractive V_2, whereas for the dielectric surface (top row) the effect is opposite. For the both cases the attractive positive surface potential V_1 increases the melting temperature (right column). At constant potential the charge density on the dielectric surface scales to the square root of the added salt content and ±25 mV corresponds to the surface charge density ±0.058 C/m^2 at 1*M* NaCl content.

for V_1 is twice as long as for V_2, for charged surfaces (Figure 2, central and right columns), the effect is longer ranged compared to the neutral surface. The length scale is determined by the inverse Debye screening length, κ, which is 0.34 nm at 1*M* NaCl and increases to 9.6 nm for 1 m*M* salt at 300 K. This increase of the screening length is the reason of observed in Figure 2 increase of the melting temperature shift as the salt concentration is lowered.

In striking agreement with our prediction,[6] Georgiadis and colleagues[7] recently observed that application of a negative surface potential enhances the DNA duplex melting. The experiment was done on oligonucleotide duplexes tethered to a gold film at a surface potential −300 mV. These conditions correspond to an ideally polarized region of the gold electrode with zero Faradaic current and thus evidence of the electrostatic mechanism of the DNA duplex destabilization. At positive surface potential, an enhanced formation of duplexes was observed in accordance with our theory. In an earlier study, Heller with co-workers[13] discovered an "electronic denaturation" of tethered to electrode DNA duplexes in conditions when electrochemical current flowed. In this case the theoretical analysis is more complex, and should include along with electrostatic interactions possible electrokinetic and electrochemical effects.

Glass Microarrays

In commonly used microarrays on glass surfaces, our estimates predict significant electrostatic effects. At equilibrium, the silica surface charge density in 1*M* sodium nitrate aqueous solution increases from zero at pH 4 to −0.24 C/m^2 at pH 9.5, corresponding to a surface potential range from 0 to −100 mV.[16] In particular, for typical hybridization conditions near pH 7, the potential is −35 and −80 mV for the salt content of 1 and 0.1*M*, respectively. Comparison with results in Figure 2 shows that for short probe–surface distances this negative surface potential may inappropriately reduce the melting temperature by tens of degrees Celsius. This decreases the number of duplexes at a given hybridization temperature and thus the sensitivity of microarray. Decrease of the equilibrium negative surface charge

(e.g., by pH adjustment or surface chemistry) may be used to improve the sensitivity.

In addition, surface charge control is required to achieve reproducibility of the microarray data. A glass surface is prone to static charging. It would be interesting to test experimentally if this random charge contributes to noise in hybridization signals and thus should be eliminated by surface discharging prior to hybridization. Below we also analyze some other limitations of current microarray designs. Using the theory developed, we consider possible improvements and suggestions for further experimental testing.

Enhancement of Match/Mismatch Discrimination

The match/mismatch discrimination ratio, characterizing selectivity of hybridization and the ability to distinguish between perfectly matched and mismatched target's sequence, may be affected considerably by the surface interactions. Because of the conformational flexibility of linker molecules, the probes are in a distribution of distances from the surface. This creates a distribution of the melting temperature, which inhomogeneously broadens the melting curve and decreases the discrimination of mismatches. Here we consider how to minimize this undesirable effect using equally distributed probes in a 0.4 nm thickness layer on a dielectric surface in 1*M* NaCl solution as an example. Figure 3A shows the melting temperature dependence on the surface charge density σ. It demonstrates that at $\sigma = +0.05$ C/m^2, T_m practically does not depend on the probe–surface distance. Hence, the inhomogeneous broadening is suppressed, and the calculated melting curve (Figure 3B) is narrower compared to the reference curve at $\sigma = -0.05$ C/m^2. As a result, the discrimination ratio (calculated for a decrease in T_m of 7°C mismatch relative to a match) increases from 4.5 to 7.

Equal Melting Temperatures of Different Probes

The known limitation of the dynamic range of microarray assays is connected with the intrinsic lesser stability and lower melting temperature of A:T compared to G:C base pairs. As a result, a probe set on a single microarray is often restricted to oligonucleotides with similar GC content in order to ensure their comparable sensitivity.[1,5,11] This limits the diversity of sequences that can be interrogated in one microarray experiment. The improved methods developed use tetraalkylammonium salts in the hybridization solution[17] and chemically modified oligonucleotides,[18,19] but are not sufficiently effective or always feasible. Results in Figure 2 suggest two

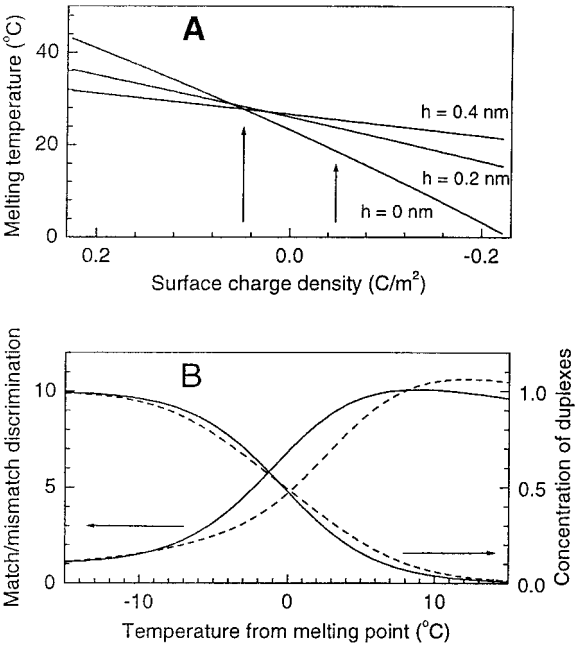

FIGURE 3 Effect of the surface charge density on the melting curve and match/mismatch discrimination ratio. (A) The melting temperature vs surface charge density curves for probes at 0, 0.2 and 0.4 nm distances from the dielectric surface in 1*M* NaCl solution. (B) The melting curves and the discrimination ratios for the surface charge density +0.05 C/m^2 (solid lines) and −0.05 C/m^2 (dashed lines) for homogeneous distribution of probes at 0 to 0.4 nm distance from surface. Near the intersection region in FIGURE 3A at $\sigma = +0.05$ C/m^2 the inhomogeneous broadening is almost eliminated making the melting curve narrower. This enhances the match/mismatch discrimination ratio at a given melting temperature up to 7 compared to 4.5.

ways to equalize the melting temperatures by individual adjustment of probe–surface distance or specific regulation of the charge density on the surface areas under different probes. In the first approach, the oligomer linkers of probe specific length may be easily attached to different probes using standard microarray fabrication techniques. The second possibility may be appropriate for arrays on metallic surface that allow separate regulation of the surface electric potential under different probes.

Melting the Secondary Structure of Assayed RNA

Application of microarrays especially for genotyping and polymorphism analysis demands effective hybridization across all the sequence of the nucleic acid target. However, experiments revealed substantial hybridization yield for only a small part of RNA sequences.[20,21]

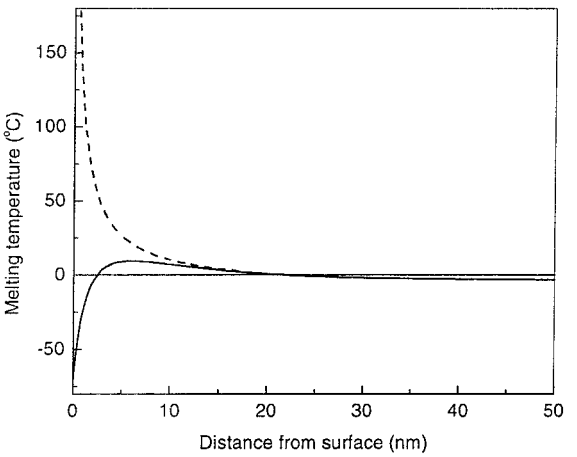

FIGURE 4 Duplex melting temperature dependence on the probe–surface distance for a positively charged $\Phi = +25$ mV dielectric (solid line) and metallic (dashed line) surface at 1 m*M* NaCl. Increase of the melting temperature near the surface makes possible effective hybridization of the premelted target nucleic acid to the tethered oligonucleotide probe located less than 20 nm from the surface.

This was attributed to the effect of secondary RNA structures, making the involved bases less accessible for duplex formation with a probe. For example, only 40% of rabbit β-globulin mRNA sequence exhibits hybridization with 17-mer probes above 10% of the highest duplex yield.[20] Similar results were reported for tRNAs showing effective heteroduplex formation for only about 10% of the sequence.[21] More efficient and homogeneous hybridization across an RNA target is expected if the secondary structure is melted. Considerable melting is known to occur at low salt conditions because a decrease from 1*M* to 1 m*M* NaCl suppresses T_m in homogeneous solution by about 40°C.[22] Despite this suppression, we show in Figure 4 that a much stronger increase of probe: RNA duplex T_m near a dielectric or metallic positively charged surface with the potential +25 mV is achieved providing the melting temperature above 0°C if the probe–surface distance is less than 20 nm. Importantly, the mechanism works by increasing target's concentration near attractive positively charged surfaces according to Eq. (2) and thus promotes only intermolecular duplex formation. It does not affect intramolecular hybridization near the surface leaving the nucleic acid targets and probes relatively more melted and structureless as needed for complete screening of target's sequence with single base resolution.

The authors thank Professors Rosina Georgiadis and Michael Hogan for stimulating conversations. AV thanks Dr. Gary F. Blackburn for a valuable discussion and Steven R. Marcuse for a careful reading of the manuscript. The authors acknowledge partial support from the NIH, Texas Higher Education Coordinating Board and the Robert A. Welch Foundation.

REFERENCES

1. Hacia, J. G. Nature Genet 1999, 21, 42–47.
2. Gerhold, D.; Rushmore, T.; Caskey C. T. Trends Biochem Sci 1999, 24, 168–173.
3. Shchepinov, M. S.; Case-Green, S. C.; Southern, E. M. Nucleic Acids Res 1997, 25, 1155–1161.
4. Forman, J. E.; Walton, I. D.; Stern, D.; Rava, R. P.; Trulson, M. O. ACS Symposium Series 1998, 682, 206–228.
5. Hughes, T. R.; Mao, M.; Jones, A. R.; Burchard, J.; Marton, M. J.; Shannon, K. W.; Lefkowitz, S. M.; Ziman, M.; Schelter, J. M.; Meyer, M. R.; Kobayashi, S.; Davis, C.; Dai, H. Y.; He, Y. D.; Stephaniants, S. B.; Cavet, G.; Walker, W. L. ; West, A.; Coffey, E.; Shoemaker, D. D.; Stoughton, R.; Blanchard, A. P.; Friend, S. H.; Linsley, P. S. Nature Biotech 2001, 19, 342–347.
6. Vainrub, A.; Pettitt, B. M. Chem Phys Lett 2000, 323, 160–166.
7. Heaton, R. J.; Peterson A. W.; Georgiadis R. M. Proc Natl Acad Sci USA 2001, 98, 3701–3704.
8. Ohshima, H.; Kondo, T. J. Colloid Interface Sci 1993, 157, 504–508.
9. Doktycz, M. J.; Moris, S. J.; Dormady, S. J.; Beattie, K. L.; Jacobson, K. B. J Biol Chem 1995, 270, 8439–8445.
10. Feig, M.; Pettitt, B. M. J Mol Biol 1999, 286, 1075–1095.
11. Fotin, A.V.; Drobyshev, A. L.; Proudnikov, D. Y.; Perov, A. N.; Mirzabekov, A. D. Nucleic Acids Res 1998, 26, 1515–1521.
12. Alberty, R. A.; Silbey, R. J. Physical Chemistry; John Wiley: New York, 1992; p 627.
13. Sosnowski, R. G.; Tu, E.; Butler, W. F.; O'Connell, J. P.; Heller, M. J. Proc Natl Acad Sci USA 1997, 94, 1119–1123.
14. Umek, R. M.; Lin, S. W.; Vielmetter, J.; Kayyem, J. F.; Yowanto, H.; Blackburn, G. F.; Farkas, D. H.; Chen, Y.-P. J Mol Diag 2001, 3, 74–84.
15. Benoit, V.; Steel, A.; Torres, M.; Yu, Y.-Y.; Yang, H.; Cooper, J. Anal Chem 2001, 73, 2412–2420.
16. Persello, J. In Adsorption on Silica Surfaces; Papirer, E., Ed.; Marcel Dekker: New York, 2000; pp 297–342.
17. Chee, M.; Yang, R.; Hubbell, E.; Berno, A.; Huang, X. C.; Stern, D.; Winkler, J.; Lockhart, D. J.; Morris, M. S.; Fodor, S. P. A. Science 1996, 274, 610–614.
18. Hoheisel, J. D. Nucleic Acids Res 1996, 24, 430–432.
19. Hacia, J. G.; Woski, S. A.; Fidanza, J.; Edgemon, K.; Hunt, N.; McGall, G.; Fodor, S. P. A.; Collins, F. S. Nucleic Acids Res 1998, 26, 4975–4982.
20. Milner, N.; Mir, K. U.; Southern, E. M. Nature Biotech 1996, 15, 537–541.
21. Mir, K. U.; Southern, E. M. Nature Biotech 1999, 17, 788–792.
22. Wetmur, J. G. Crit Rev Biochem Mol Biol 1991, 26, 227–259.